Carrier thermalization versus phonon-assisted relaxation in quantum-cascade lasers: A Monte Carlo approach

Carrier thermalization versus phonon-assisted relaxation in quantum-cascade lasers: A Monte Carlo approach

Rita Claudia Iotti and Fausto Rossi

Citation: Appl. Phys. Lett. **78**, 2902 (2001); doi: 10.1063/1.1370537
View online: http://dx.doi.org/10.1063/1.1370537
View Table of Contents: http://apl.aip.org/resource/1/APPLAB/v78/i19
Published by the American Institute of Physics.

Carrier thermalization versus phonon-assisted relaxation in quantum-cascade lasers: A Monte Carlo approach

Rita Claudia Iotti[a] and Fausto Rossi
Istituto Nazionale per la Fisica della Materia (INFM) and Dipartimento di Fisica, Politecnico di Torino, Corso Duca degli Abruzzi 24, 10129 Torino, Italy

(Received 13 December 2000; accepted for publication 9 March 2001)

In this letter, we present a microscopic analysis of the hot-carrier dynamics governing intersubband light-emitting devices. In particular, a global Monte Carlo simulation scheme is proposed in order to directly access details of the three-dimensional carrier relaxation, without resorting to phenomenological parameters. The competition between intercarrier thermalization and phonon-assisted relaxation in quantum-cascade lasers is investigated and their relative importance on device performance is clearly identified. © *2001 American Institute of Physics.*
[DOI: 10.1063/1.1370537]

Beside their fundamental interest, hot-electron relaxation processes play a crucial role in determining the operation efficiency of many semiconductor-based quantum devices. A typical example is represented by quantum-cascade lasers (QCLs).[1] QCLs are unipolar solid-state devices in which the principles of quantum engineering are heavily exploited: coherent-light generation in the infrared spectral region is obtained, as the name suggests, via an electronic cascade along the energy-level staircase of a sequence of coupled quantum wells. A proper tailoring of optical matrix elements and relaxation times is crucial to achieve a population-inversion regime. This can be done by designing the intersubband energy separations to benefit of an energy-selective channel by which electrons can dissipate their energy: the optical-phonon-emission cascade.

Since their appearance, QCLs have been the subject of significant experimental development and relevant theoretical interest. The various theoretical models which have been proposed up to now,[2] however, resort to macroscopic rate equations to describe the carrier dynamics, whose application require a strict hypothesis on the carrier distribution function, i.e., on the microscopic details of the relaxation process. An attempt to check the validity of these fundamental assumptions has recently been made by Harrison,[3] by directly comparing intra- and intersubband electron–electron and electron–longitudinal-phonon scattering rates. As pointed out in Ref. 3, however, this approach does not provide access to the dynamical evolution of the electron distribution function and only microscopic simulations can give a definite answer.

The main difficulty a quantitative study of QCLs has to face is the inadequacy of the usual approach, which treats intersubband lasers by analogy with an n-level atomic system. Rather than within a multilevel system, the electron dynamics in QCLs occurs within a multisubband structure, and the existence of transverse degrees of freedom, i.e., the in-plane dynamics, should be properly taken into account. One of the most suitable approaches to describe carrier dynamics within a kinetic or Boltzmann-like formulation is the Monte Carlo (MC) method:[4] It allows us to take into account intra- as well as intersubband scattering processes on equal footing and to include a large variety of scattering mechanisms. The aim of this letter is to provide quantitative insight into the carrier dynamics in QCLs and to address the reliability of macroscopic descriptions. This is achieved by means of a fully three-dimensional analysis based on a suitable nonconventional multisubband MC simulation scheme.

QCLs are complex structures, whose core is made up of repeated stages of active regions, sandwiched between electron-injecting and collecting regions.[1] As a starting point of our MC approach, we evaluate—within a self-consistent Schrödinger–Poisson scheme in an envelope-function framework—[5,6] the set of three-dimensional single-particle electron states $|\mathbf{k},\nu\rangle$ corresponding to the generic QCL stage λ, e.g., the active region plus the collector/injector in the presence of the applied bias (see Fig. 1). Given such carrier states, we consider the ideal multi-quantum-well (MQW) structure obtained as an infinite repetition of this QCL periodicity region. Within such an extended scheme, the time evolution of the carrier distribution function $f_{\mathbf{k}\alpha}$ is governed by the following Boltzmann-like equation:

$$\frac{d}{dt} f_{\mathbf{k}\alpha} = \sum_{\mathbf{k}'\alpha'} \sum_{s} \left[P^{s}_{\mathbf{k}\alpha,\mathbf{k}'\alpha'} f_{\mathbf{k}'\alpha'} - P^{s}_{\mathbf{k}'\alpha',\mathbf{k}\alpha} f_{\mathbf{k}\alpha} \right], \tag{1}$$

where $\alpha \equiv (\lambda,\nu)$, $P^{s}_{\mathbf{k}\alpha,\mathbf{k}'\alpha'}$ is the scattering probability for a process connecting the state with in-plane wavevector $\mathbf{k}$ in the νth subband of the λth stage, to the state $\mathbf{k}'\nu'$ of the λ'th stage, and s labels the different scattering mechanisms considered, e.g., carrier–phonon, carrier–carrier, etc. To ''close the circuit,'' we impose periodic boundary conditions limiting the interstage ($\lambda' \neq \lambda$) coupling to just nearest-neighbor scattering ($\lambda' = \lambda \pm 1$). In view of the translational symmetry, we are allowed to simulate the carrier transport over the central—i.e., $\lambda = 0$—stage only. Every time a carrier in state ν undergoes an interstage scattering process (i.e., 0, $\nu \rightarrow \pm 1$, ν', it is properly reinjected into the central region $(0,\nu \rightarrow 0,\nu')$ and the corresponding electron charge $\pm e$ will contribute to the current through the device.[7]

[a]Also at: Scuola Normale Superiore, Piazza dei Cavalieri 7, 56126 Pisa, Italy; electronic mail: iotti@athena.polito.it

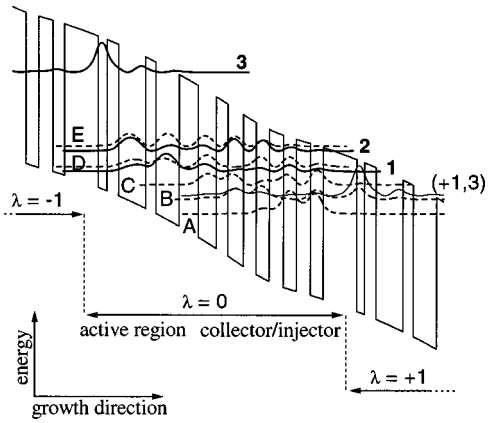

FIG. 1. Schematic representation of the conduction-band profile along the growth direction for the QCL structure of Ref. 8. The MQW is biased by an electric field of 48 kV/cm. The levels $\nu=1, 2, 3$ and $\nu=$A, B, C, D, E in the active and collector regions (full and dashed lines, respectively) of the simulated stage ($\lambda=0$) are also plotted together with the corresponding probability densities. The replica of level 3 in the following stage $\lambda=+1$ is shown for clarity as well. The separation between levels 1 and 2 matches the optical-phonon energy ($\hbar\omega_{\mathrm{LO}}\simeq 36$ meV) and the stage length is 453 Å (the figure is in scale).

We have applied the proposed simulation scheme to MQWs forming the active region of state-of-the-art QCLs. In particular, we have investigated the GaAs/(Al,Ga)As-based diagonal-configuration device of Ref. 8, schematically depicted in Fig. 1. Here, the energy levels and probability densities of various electron states within the simulated stage ($\lambda=0$) are also plotted: They correspond to the device active region (full line, $\nu=1, 2, 3$) as well as to the collector region (dashed line, $\nu=$A, B, C, D, E). To properly model charge transport along the heterostructure growth direction, the relevant interaction mechanisms have been included at a kinetic level in our simulation, namely, all various intra- as well as intersubband carrier-optical-phonon and carrier–carrier scattering processes.

In order to focus on the relative weight of the carrier–carrier and carrier–phonon competing energy-relaxation channels, we have plotted in Fig. 2 the steady-state carrier distribution as a function of the in-plane energy, for different carrier densities, ranging from 3.9×10^{8} cm^{-2} [case (a)], to 3.9×10^{11} cm^{-2} [case (c)]. Figure 2(d) corresponds to the simulation performed in the absence of intercarrier scattering [here, the carrier density is the same as in Fig. 2(c)]. For simplicity, the results are shown for the carrier distribution function in subband $\nu=1$ only, but electrons in all the remaining subbands behave in a similar way: as for the case of ultrafast relaxation of photoexcited carriers,[9] the carrier distribution function evolves from a phonon-replica scenario (a) to a thermalized distribution (c). Indeed, for low carrier densities, intercarrier scattering plays a very minor role and the electrons relax their energy via a cascade of successive optical-phonon emissions ($\hbar\omega_{\mathrm{LO}}\simeq 36$ meV); for high carrier densities carrier–carrier scattering is more effective in setting up a heated Maxwellian distribution, with a given temperature T_{ν}. This is a well-known trend which results from the screened-Coulomb nature of the carrier–carrier interaction potential.[4] The absolute density value corresponding to the transition between these two different regimes, however, depends on the heterostructure details and can be obtained

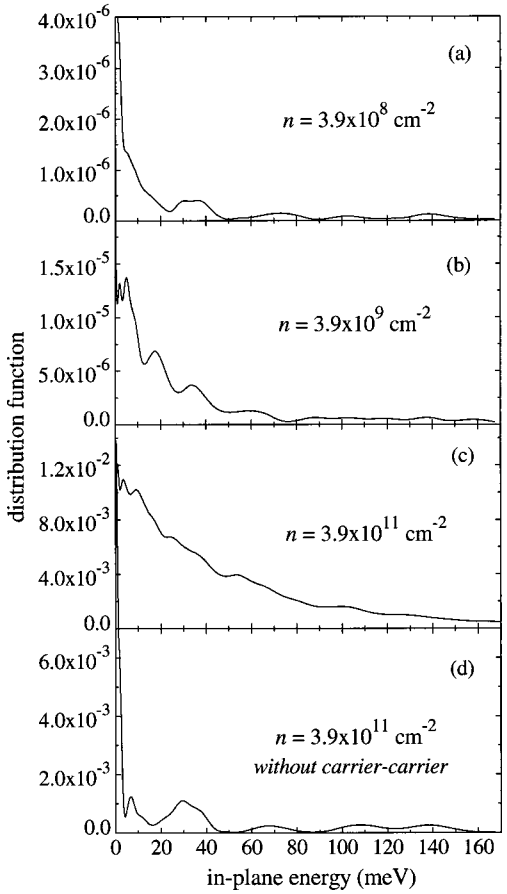

FIG. 2. Electron distribution function vs in-plane energy, for carriers in subband 1. Simulations are performed for the MQW structure of Fig. 1 at diverse carrier densities: (a) 3.9×10^{8} cm^{-2}; (b) 3.9×10^{9} cm^{-2}; (c) 3.9×10^{11} cm^{-2}; and (d) without carrier–carrier scattering.

only after performing a direct simulation. Our results clearly show that, for typical operating conditions (sheet density$=3.9\times10^{11}$ cm^{-2}), electrons in QCLs thermalize within each subband. This confirms one of the main conclusions drawn by Harrison.[3] However, we stress that this behavior is strongly density dependent, as we expect from the theory and correctly recover from the simulations in Fig. 2. Contrary to what is stated in Ref. 3, while the total carrier–carrier scattering rate is quite density independent, its net effect on the carrier distribution is known to depend strongly on density: At low density we mainly deal with ''forward scattering'' processes, which are quasielastic and thus do not provide a relevant intrasubband energy exchange required by proper thermalization.

Temperatures corresponding to the diverse subbands vary in a quite narrow range ($T_{\nu}=600$–750 K), as shown in Fig. 3.[10] Again, the role of the electron–electron interaction is crucial in setting up this behavior. As pointed out in Ref. 3, this can be mainly ascribed to *bi-intrasubband* scattering processes, i.e., intercarrier scattering processes coupling electrons in different subbands, without changing their principal quantum number ν. They provide, in fact, a very efficient way of redistributing excess kinetic energy in order to achieve a common effective temperature. Such temperature is about 700 K, compared to a lattice temperature of 77 K assumed in the simulation. This heating is a clear fingerprint of a strong hot-carrier regime: the carrier system is not able

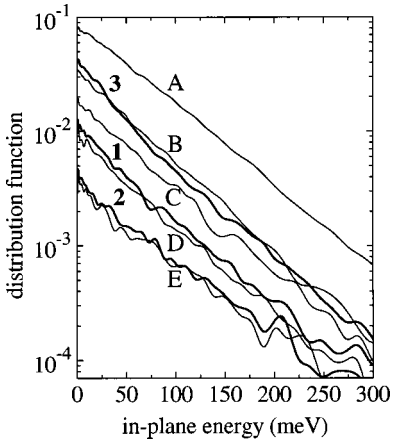

FIG. 3. Electron distribution function vs in-plane energy, for carriers in subbands $\nu=1, 2, 3$ and $\nu=$A, B, C, D, E of the MQW structure in Fig. 1. Sheet density$=3.9\times10^{11}$ cm^{-2}. The slope of each curve provides an estimate of the effective carrier temperature T_ν, which ranges from 600 to 750 K.

to dissipate—via optical-phonon emission—the relatively large amount of energy provided by the applied bias.

Particle and energy redistribution within the various subbands, due to the carrier–carrier interaction, is of fundamental importance in determining device performance as well. Figure 4 reports the gain spectra corresponding to the 3→2 optical transition obtained from simulated experiments performed with (solid curve) and without carrier–carrier interactions (dashed curve). The Lorentzian linewidth is determined self-consistently within our kinetic scheme, through the calculated scattering rates. The carrier–carrier contribution to the spectral broadening is corrected by a phenomenological factor, which increases with electron density and reproduces the effect of in-scattering terms in the polarization

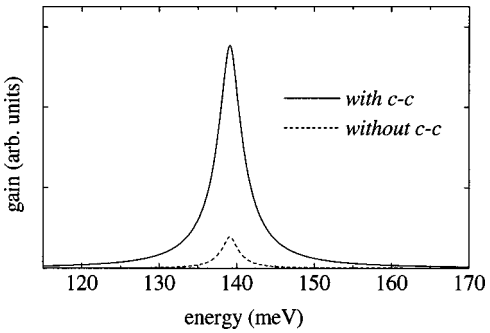

FIG. 4. Gain spectra of the 3→2 optical transition for the MQW structure of Fig. 1. Full line: carrier–phonon as well as carrier–carrier interactions are included in the simulation; dashed line: with carrier–phonon interaction only.

dynamics.[9] The positive values of both gain spectra show that a regime of population inversion between the highest ($\nu=3$) and intermediate level ($\nu=2$) of the active region (see Fig. 1) is eventually established in both cases. Intercarrier scattering, however, does strongly increase the gain efficiency.

In conclusion, the proposed MC simulation scheme has allowed the quantitative investigation of the interplay between phonon-assisted energy relaxation and carrier–carrier intra-, as well as intersubband, thermalization. Our analysis shows that the operation of the QCL structure of Ref. 8 (sheet density 3.9×10^{11} cm^{-2} per period) is dominated by hot-electron effects and presents a pronounced nonequilibrium intersubband carrier population. Inspite of the intrasubband thermalization and of the strong intersubband in-plane energy exchange, at stationary conditions, the desired regime of population inversion between the highest and the intermediate level of the active region is properly achieved.

Discussions with F. Beltram, C. Sirtori, and A. Tredicucci are gratefully aknowledged. This work has been partially supported by the European Commission through the Brite Euram UNISEL project and the FET WANTED project.

[1] J. Faist, F. Capasso, D. L. Sivco, C. Sirtori, and A. Y. Cho, Science **264**, 553 (1994); G. Scamarcio, F. Capasso, C. Sirtori, J. Faist, A. L. Hutchinson, D. L. Sivco, and A. Y. Cho, *ibid.* **276**, 773 (1997); C. Gmachl, A. Tredicucci, D. L. Sivco, A. L. Hutchinson, F. Capasso, and A. Y. Cho, *ibid.* **286**, 749 (1999).

[2] See, e.g., V. B. Gorfinkel, S. Luryi, and B. Gelmont, IEEE J. Quantum Electron. **32**, 1995 (1996); L. Friedman and R. A. Soref, J. Appl. Phys. **83**, 3480 (1998).

[3] P. Harrison, Appl. Phys. Lett. **75**, 2800 (1999).

[4] See, e.g., C. Jacoboni, and P. Lugli, *The Monte Carlo Method for Semiconductor Device Simulations* (Springer, Wein, 1989).

[5] This can be viewed as an extension of the Monte Carlo scheme previously proposed, but limited to the active region only [R. C. Iotti and F. Rossi, Appl. Phys. Lett. **76**, 2265 (2000).] The present approach, however, does not require any phenomenological assumption on injection/loss mechanisms. This allows us to consistently simulate carrier relaxation processes, without resorting to external parameters. Corrections to the Schrödinger–Poisson self-consistent field due to hot carriers can be neglected for these relatively low densities.

[6] S. Barbieri, F. Beltram, and F. Rossi, Phys. Rev. B **60**, 1953 (1999).

[7] In this charge-conserving scheme the current density across the whole structure is a pure output of the simulation. The current/voltage characteristics of the semiconductor heterostructure can thus be obtained within a purely microscopic description.

[8] C. Sirtori, P. Kruck, S. Barbieri, P. Collot, and J. Nagle, Appl. Phys. Lett. **73**, 3486 (1998).

[9] T. Kuhn, in *Theory of Transport Properties of Semiconductor Nanostructures*, edited by E. Schöll (Chapman and Hall, London, 1998), p. 173.

[10] It should be noted that this temperature T_ν has nothing to do with the effective temperature invoked in a macroscopic n-level description, which becomes negative in the case of population inversion.